Received September 2001
Revised October 2002
Accepted November 2002

Heat transfer to pulsating turbulent flow in an abrupt pipe expansion

S.A.M. Said, M.A. Habib and M.O. Iqbal
Department of Mechanical Engineering, King Fahd University of Petroleum and Minerals, Dhahran, Saudi Arabia

Keywords *Turbulent flow, Heat transfer, Thermal expansion*

Abstract *A numerical investigation aimed at understanding the flow and heat transfer characteristics of pulsating turbulent flow in an abrupt pipe expansion was carried out. The flow patterns are classified by four parameters; the Reynolds number, the Prandtl number, the abrupt expansion ratio and the pulsation frequency. The influence of these parameters on the flow was studied in the range* $10^4 < Re < 5 \times 10^4$, $0.7 < Pr < 7.0$, $0.2 < d/D < 0.6$ *and* $5 < f < 35$. *It was found that the influence of pulsation on the mean time-averaged Nusselt number is insignificant (around 10 per cent increase) for fluids having a Prandtl number less than unity. This effect is appreciable (around 30 per cent increase) for fluids having Prandtl number greater than unity. For all pulsation frequencies, the variation in the mean time-averaged Nusselt number, maximum Nusselt number and its location with Reynolds number and diameter ratio exhibit similar characteristics to steady flows.*

Nomenclature

A = pipe wall area
a = constant
C_μ = constant in turbulence model
C_f = constant
d = upstream pipe diameter
D = downstream pipe diameter
E = roughness parameter (law of the wall)
f = frequency
h = local heat transfer coefficient
H = enthalpy
H = step height $\{(D\text{-}d)/2\}$
k = kinetic energy of turbulence
L = length of the downstream section
l = length scale
$\dot{m}$ = mass flow rate
Nu = Nusselt number based on downstream dimensions
P = mean static pressure
Pr = Prandtl number
q'' = local heat flux
Q_w = wall heat transfer
r = upstream pipe radius
R = downstream pipe radius
Re = Reynolds number = $U_m D/\nu$
S_ϕ = source of variable ϕ
t = time in a cycle of pulsation
T = total time of cycle
T = absolute temperature
U, V = time averaged velocity components in equation (1)
u, v = velocity components at the wall
$U(r)$ = steady state inlet velocity profile
$u(r)$ = pulsating velocity profile at the inlet to abrupt expansion
x = axial coordinate
y = radial distance from the center of the pipe

The support of King Fahd University of Petroleum and Minerals in conducting this study is acknowledged.

International Journal of Numerical Methods for Heat & Fluid Flow
Vol. 13 No. 3, 2003
pp. 286-308

0961-5539
DOI 10.1108/09615530310464517

Greek symbols

α = amplitude of pulsation
Γ_φ = exchange coefficient for ϕ
ε = dissipation rate of turbulence energy
κ = von Karman constant (law of the wall)
μ = viscosity
ν = kinematic viscosity
ρ = density
ϑ = general dependant variable

Subscripts

b = bulk
fd = fully developed
l = laminar
in = inlet
max = maximum
p = pulsating
p = nearest node to the wall in equation (12)
s = steady
t = turbulent
w = wall

Superscript

- = average

Introduction

The turbulent flow downstream of an axisymmetric sudden expansion has been of interest to many investigators due to its theoretical and practical importance. Such geometry is encountered in many industrial applications such as heat exchangers, combustion chambers and chemical mixing equipment. Several experimental and theoretical investigations have been conducted to study the flow field and heat transfer characteristics of such geometry for steady-state flows. Experimental investigations include those of Amano *et al.* (1983), Baughn *et al.* (1984, 1987, 1989), Dallen back *et al.* (1987), Krall and Sparrow (1966), Vogel and Eaton (1985), and Zemanic and Dougall (1970), while numerical investigations include those of Amano (1983), Chieng and Launder (1980), Habiband McEligot (1982) and Valencia *et al.* (1996). Those experimental and numerical investigations showed that the local heat transfer coefficients in the separated, reattached and redevelopment regions were several times (5 to 9 times) higher than those for a fully developed flow in a pipe having the same diameter as the downstream. The heat transfer enhancement, both maximum and average values of heat transfer coefficients, increased strongly as the abrupt expansion ratio increased. The location of the maximum heat transfer coefficient moved downstream as the abrupt expansion ratio increased and the peak values of Nusselt number correlated fairly well in terms of the Reynolds number based on the upstream pipe diameter irrespective of the expansion ratio. Previous theoretical studies concerned with laminar flows provide heat transfer enhancement through the use of fins and pulsating components. These include the work of Cho and Hyun (1989), Hammad and Vrandis (1998), Kim and Yang (1998), Valencia and Hinojosa (1997) and Valencia *et al.* (1996). Valencia and Hinojosa (1997), in their numerical solutions of pulsating flow and heat transfer characteristics in channel with a backward-facing step, found that wall shear rate in the separation zone

varied markedly with pulsatile flow and wall heat transfer remained relatively constant. The time-average pulsatile heat transfer at the wall was greater as with the steady flow for same Reynolds number. Cho and Hyun (1989) found that the conventional Reynolds analogy of skin friction and heat transfer holds for low frequency but is not applicable at high frequency for motion and heat transfer studies of flow containing a pulsating component.

As can be seen from the literature review, the problem of steady turbulent and laminar flows in sudden pipe expansion has received much attention. However, no work has been reported on heat transfer characteristics in the separation regions of a pulsating turbulent flow in sudden pipe expansions. In this study, a numerical investigation aimed at understanding the flow and heat transfer characteristics for the pulsating turbulent flow in abrupt pipe expansion is carried out.

Problem formulation

The present study is based on the numerical solution of the two-dimensional form of the time-averaged Navier-Stokes equations. The two-equation k-ε model was used in the present calculations. Turbulent viscosity is defined by the high Reynolds number version of the k-ε model. The physical properties were assumed to be constant. Hence, the governing equations for the present flow configuration can be written in general form as:

$$\frac{\partial \rho\varphi}{\partial t} + \frac{\partial}{\partial x}\left(\rho U\varphi - \Gamma_\varphi \frac{\partial \varphi}{\partial x}\right) + \frac{1}{r}\frac{\partial}{\partial r}\left(\rho r V\varphi - \Gamma_\varphi r \frac{\partial \varphi}{\partial r}\right) = S_\varphi \tag{1}$$

where φ is the dependent variable, Γ is the diffusion coefficient and S is the source term.

Inlet and boundary conditions

Inlet

A fully developed inlet velocity profile is used for steady turbulent flows. The walls are maintained at a constant temperature which is higher than that of the fluid and are treated as no-slip.

$$U(r) = U_{\text{in}}\left(1 - \frac{y}{r}\right)^{\frac{1}{7}} \tag{2}$$

$$T = T_{\text{in}} \tag{3}$$

For the pulsating turbulent flow, the fully developed inlet velocity profile is used and the axial velocity component is assumed to be sinusoidal in time as given by:

$$u(r) = U(r)(1 + \alpha \sin(f \cdot t)) \tag{4}$$

where U_{in} is the steady-state inlet velocity, α is the amplitude of oscillation, f is the frequency and t is the time.

Values of k and ε are not known at the inlet, but, they are approximated (Rodi, 1984) as:

$$k = \lambda \bar{u}^2 \tag{5}$$

where $\bar{u}$ is the average inlet velocity and λ is a constant equal to 0.03, and

$$\varepsilon = C_\mu \frac{k^{\frac{3}{2}}}{l} \tag{6}$$

where $l = aR$ with R as the radius of the downstream pipe and a as constant ($a = 0.03$)

Walls

The boundary conditions for the steady-state flow and unsteady flow are given as:

$$u = 0, \quad v = 0, \text{ and } \quad T = T_w \tag{7}$$

The value of the kinetic energy of turbulence near the wall, k_p is calculated from the transport equation for k with the flux of energy to the solid wall set at zero. The corresponding value of ε is calculated from equation (6) where $l = C_\mu \kappa y_p$.

The heat transfer coefficient was calculated as follows:

$$h = \frac{\dot{Q}_w}{[A(T_w - T_b)]} \tag{8}$$

where A is the wall area and T_b is the bulk temperature and is given by:

$$T_b = \frac{\int_0^D U(r) T \, dy}{\int_0^D U(r) \, dy} \tag{9}$$

and T_w is the wall temperature.

$\dot{Q}_w$ is the wall heat transfer and is calculated as follows:

$$\dot{Q}_w = \frac{\frac{\mu_1 |H_w - H_p|}{y_p}}{\frac{y_p^+}{(\bar{U}_p^+ + P_f)}} \tag{10}$$

where

$$U_{\mathrm{p}}^{+} = \frac{1}{\kappa}\ln(Ey_{\mathrm{p}}^{+}),$$

$$y_{\mathrm{p}}^{+} = C_{\mu}^{0.25}k_{\mathrm{p}}^{0.25}y_{\mathrm{p}}/\nu, \text{ and}$$

$$P_f = C_f\left[\frac{\mathrm{Pr_l}}{\mathrm{Pr_t}-1}\right]\left(\frac{\mathrm{Pr_t}}{\mathrm{Pr_l}}\right)^{\frac{1}{4}}$$

The subscript p refers to the node nearest to the wall and E, κ, and C_f are constants ($\kappa = 0.4187$, $\mathrm{C}_f = 9.24$, and $E = 9.793$). The average Nusselt number is given by:

$$\bar{N}u = \int_0^L \frac{\bar{N}u\,\mathrm{d}x}{L} \tag{11}$$

Outlet

A long domain of approximately 50 diameters was chosen to minimize the boundary influence of the downstream conditions. Thus, at the outlet, all variables are assumed to be fully developed with zero-axial gradient condition:

$$\frac{\partial\varphi}{\partial x} = 0 \tag{12}$$

and across a symmetric boundary, all normal gradients are zero in addition to zero cross flow.

$$\left(\frac{\partial\varphi}{\partial r}\right)_{r=0} = 0 \tag{13}$$

Numerical analysis

A discretized version of the governing equation (equation (1)) is derived by integrating it over a control volume with surface fluxes formulated by a quadratic upwind interpolation method (Versteeg and Malalasekera, 1995) and solved by the SIMPLE algorithm (Patankar, 1980). Applying this integration procedure to all control volumes and for all the dependent variables in field results in an algebraic equation system. The solution procedure is implicit in space coordinates and explicit in time coordinate. To establish a pulsating flow, the flow velocity at the inlet to the abrupt expansion is varied sinusoidally as given by equation (4). The solution converges at each time step before proceeding to the next time step. The time resolution is taken such that each pulsation period is divided into 20 time steps. Converged steady state solution is used as an initial condition. As the flow field is symmetric, the analysis was performed in only half of the domain.

The validity of the numerical calculations is verified through grid-dependence tests and comparisons with experimental results for steady turbulent flow. The grid points are clustered in the radial direction so that the finer spacing is formed near the wall and at the boundary of the recirculation region. A typical grid system is shown in Figure 1(a). Non-uniform grids of 29×24 were employed. Grid independence tests were made for the predicted values of the velocity profiles and the Nusselt number. Tests for grid independence were made in comparison with the data of Habiband Whitelaw (1980) for two coaxial jets. Figure 1(b) shows that increasing the grid from 24×18 to 30×22 has no effect on the predicted velocity field. Figure 1(c) shows that increasing the grid from 27×20 to 29×24 has maximum error of only 1.3 per cent rather than 7 per cent for grid increase from 21×15 to 27×20. Extrapolation of these data shows that the error in the the predicted Nusselt number of the presently used grid of 29×24 will be much less than 0.3 per cent as a numerical error. The convergence tolerance was set at 10^{-4} for flow variables and 10^{-4} for enthalpy.

To validate the numerical calculations, the computational results for steady flow were compared with experimental results available in the literature. Figure 2 shows comparison between the present computational results and the experimental results of Stieglmer *et al.* (1989) for the radial distribution of the axial velocity at different downstream axial positions. As can be seen, there is a close agreement with the experimental results. Figure 3(a)-(c) shows the comparison between the present numerical results for the local Nusselt number downstream of an abrupt pipe expansion and the experimental results reported by Zemanic and Dougall (1970). Close agreement is exhibited in trend and values for a Reynolds number of 10,000 to 17,990. A significant difference is observed when Reynolds numbers is increased to 47,600. As reported by Zemanic and Dougall, the values of the Nusselt number (for this case) appeared anomalously low which led to rerun. The results for the rerun were within ± 10 per cent of the measured values. We may therefore conclude that, given this degree of experimental variation and computational approximation together with the effect of the turbulence model used, the computed results shown in Figure 3 are in close agreement with the measured values. Other comparisons of the predicted reattachment length and the maximum Nusselt number with experimental data are presented in Table I and Figure 4(a) and (b). Table I shows the influence of Reynolds number on the location of maximum Nusselt number. The location of the peak value of the Nusselt number shifts upstream from 10 to 8.5 step height as the Reynolds number increases from 10,000 to 50,000. This behavior is in accordance with the experimental results of Baughn *et al.* (1984) and Zemanic and Dougall (1970).

Results and discussion

The first set of results pertains to the streamlines for pulsating flows. Figure 5 shows the streamlines of the air flow at Reynolds number (Re_D) 50,000 and a

(a) Computational grid for the sudden expansion

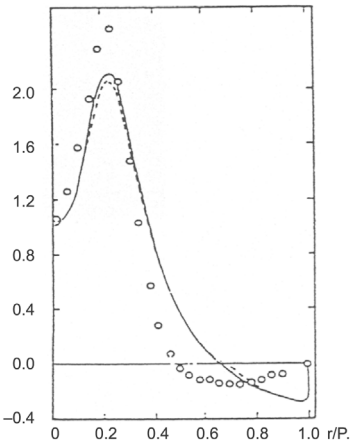

(b) Effect of Grid Size on the Mean Velocity Values along the Radius. ---, 18x24; ____, 24x18; __ . ___, 30x22; o, Experimental Data, Habib and Whitelaw (1980)

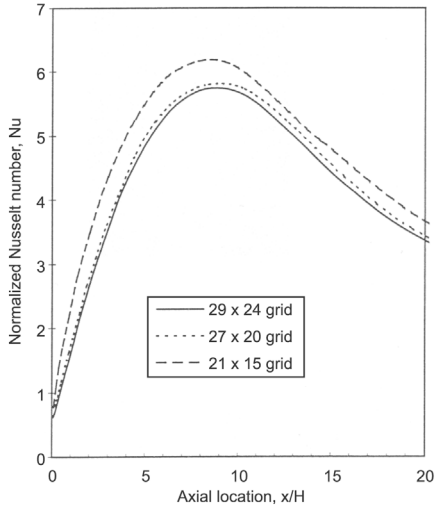

(c) Grid independence test; Re = 47800, d/D = 0.43 and Pr = 0.7

Figure 1.

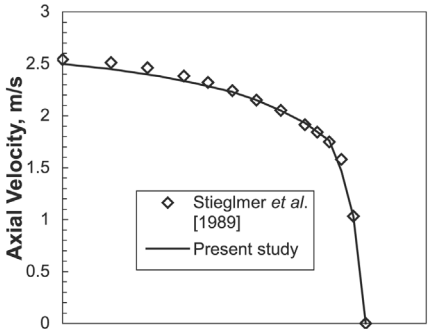

(a) 0 mm from the step

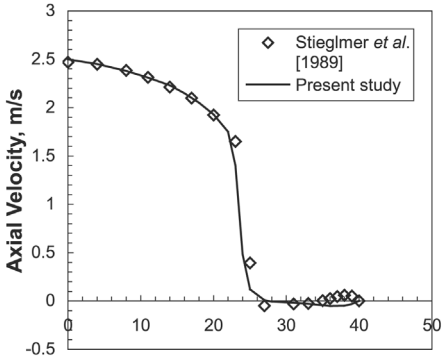

(b) 5 mm from the step

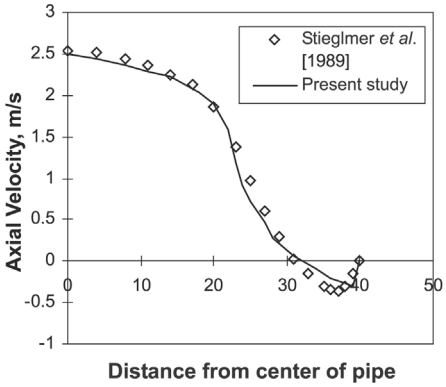

(c) 40 mm from the step

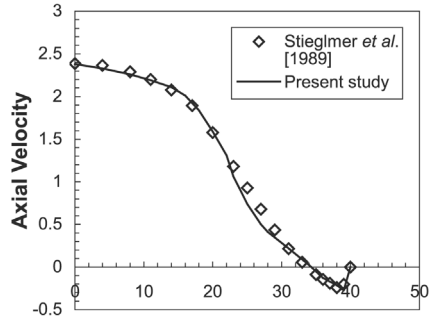

(d) 80 mm from the step

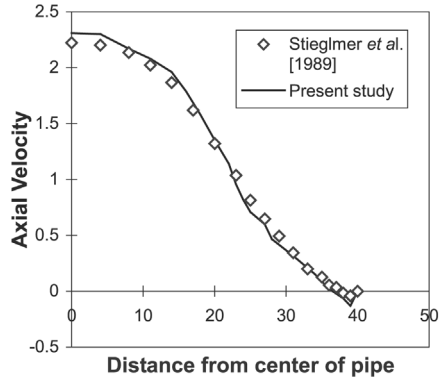

(e) 120 mm from the step

Figure 2.
Radial profiles of axial velocity component

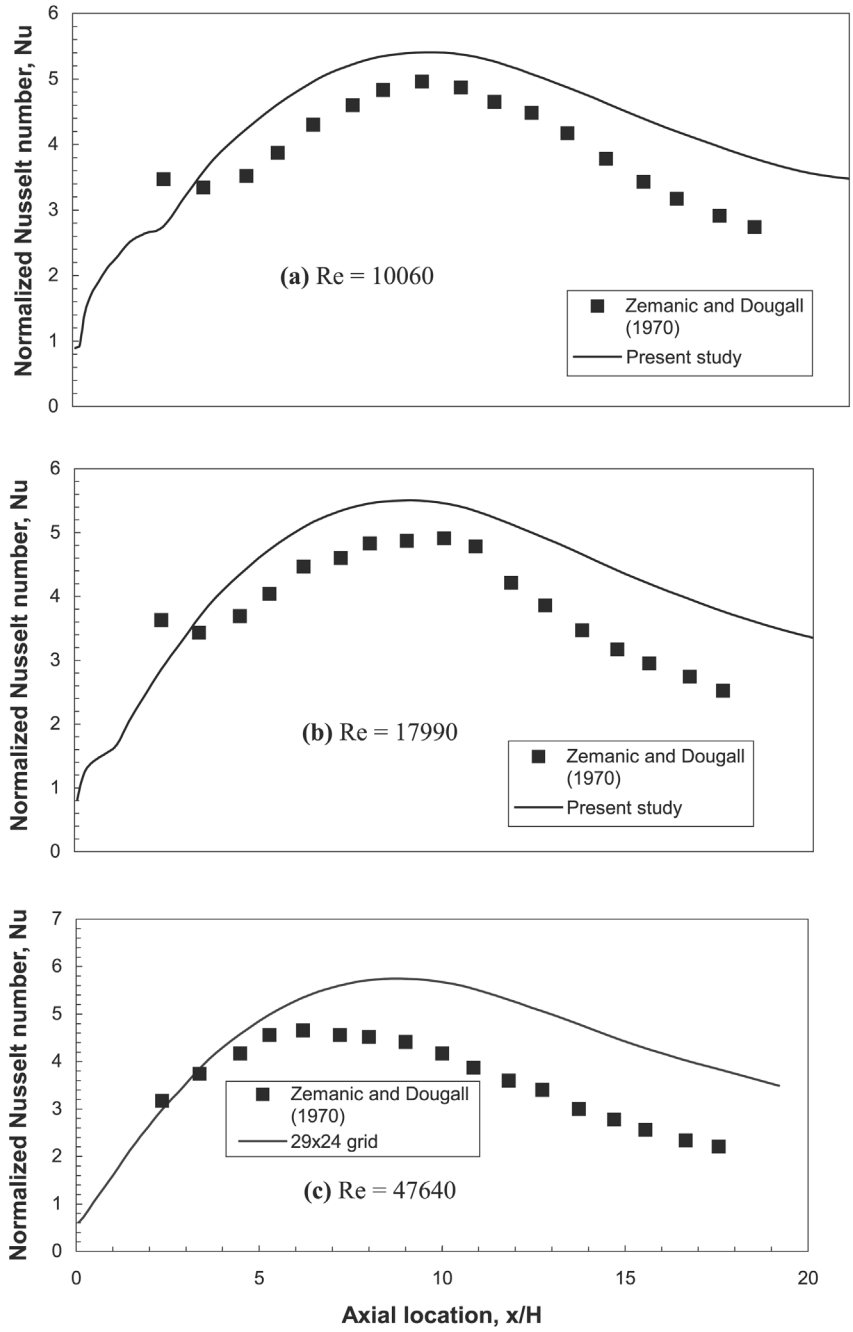

Figure 3.
Variation of local Nusselt number at different Reynolds number, $d/D = 0.43$, $Pr = 0.7$

Investigator	Re	Reattachment length (x/H)
Zemanic and Dougall (1970), $d/D = 0.43$, Pr = 0.7	4,180	9
	7,040	9
	10,060	9
	17,990	10
	47,640	6.2
	66,260	5.9
Baughn *et al.* (1984), $d/D = 0.4$, Pr = 0.7	4,310	12
	7,120	12
	17,310	10
	44,540	9
Present work, $d/D = 0.43$, Pr = 0.7	7,040	10
	10,060	9.73
	17,990	9.53
	47,640	8.5

Table I. Comparison of reattachment lengths (x/H) at different Reynolds numbers

diameter ratio (d/D) of 0.5 at different times in a pulsation cycle for a pulsation frequency of 10 Hz. Since the flow is axi-symmetric only half of the pipe is shown in the figure. As can be seen, there is a recirculating zone immediately after the step. The flow reattaches at a certain distance downstream from the abrupt expansion. The value of the streamline at the boundary of the recirculating zone corresponds to a stream function value of unity, while the value of the streamline at the centerline of the pipe corresponds to a stream function value of zero. As can be seen recirculation occurs immediately downstream from the abrupt expansion and the recirculation-zone length varies with time. The reattachment length decreases slightly with time during the first and fourth quarter of the cycle and increases again during the second and third quarter of the cycle. This is attributed to the change in the magnitude of velocity with time during each cycle. Figure 6 shows the variation of the local Nusselt number along the axial location at different times in a pulsation cycle. As can be seen, the location of the maximum Nusselt number (expected at the reattachment point) varies in the same manner as the reattachment length as it decreases in the first and fourth quarters of the cycle and increases again in the second and third quarters of the cycle.

The second set of results pertains to the effect of the Prandtl number on the local Nusselt number for pulsating flows. Figure 7(a) and (b) shows the time-averaged local Nusselt number versus the axial location x/H for two values of the Prandtl number 0.7 and 7.0. The plots exhibit a similar trend to the steady-state case. The local Nusselt number downstream from an abrupt expansion increases to a maximum value and then decreases to the fully developed value as discussed earlier. As can be seen from Figure 7(a), the effect of frequency on the Nusselt number is insignificant for fluids having the Prandtl number in the

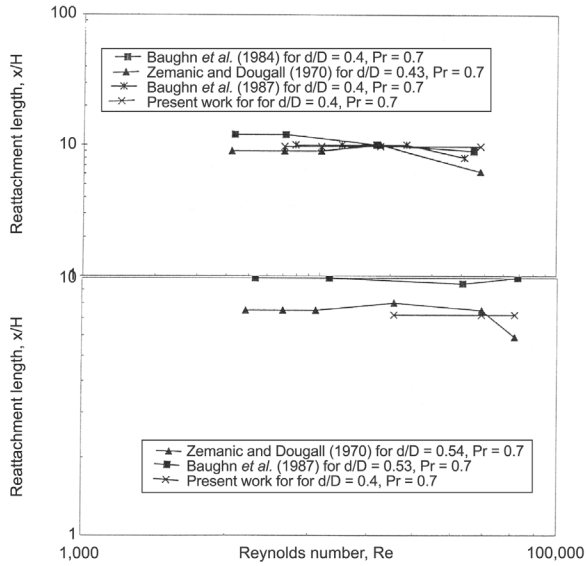

(a) Comparison of the measured and calculated Reattachment length at different Reynolds numbers

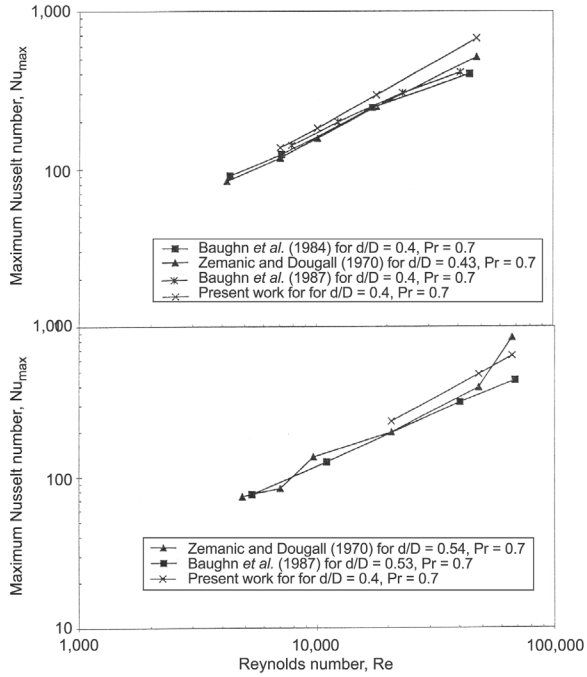

(b) Variation of the Maximum Nusselt number with Reynolds number

Figure 4.

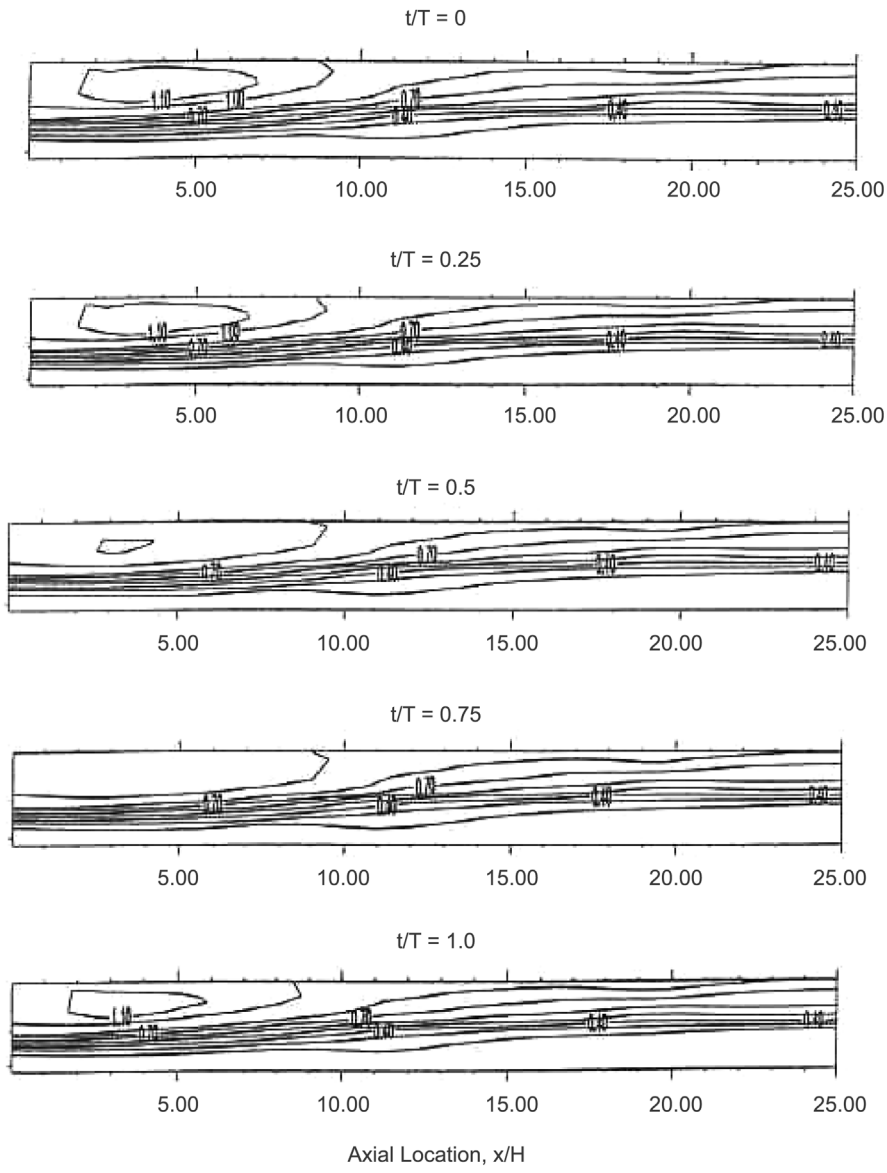

Figure 5.
Streamlines plot for a cycle of pulsation at Re = 50,000, $d/D = 0.5$, $f = 10$ Hz, and Pr = 0.7

order of 1 or less. This effect is appreciable for fluids of higher Prandtl numbers ($Pr > 1$) as can be seen from Figure 7(b). Increase in the Reynolds number has negligible effect on the values of the local Nusselt number for all the values of pulsation frequency considered in the present study (see Figure 7(a) and (b)).

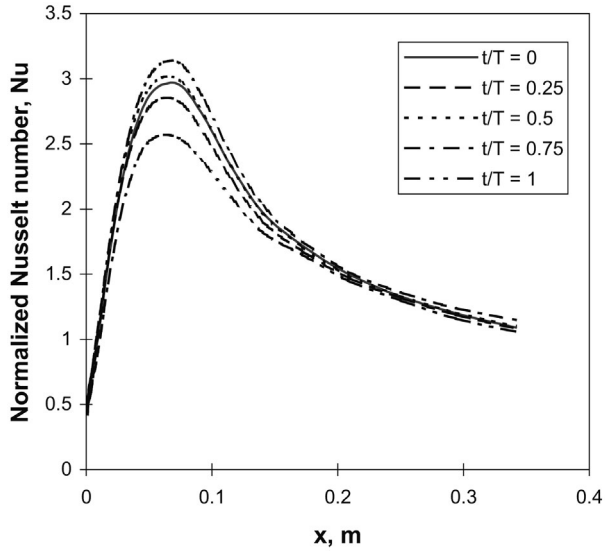

Figure 6.
Local Nusselt number at different time step in a cycle of pulsation at Re = 50,000, $f = 10$ Hz, $d/D = 0.5$, and Pr = 0.7

The third set of results pertains to the time-averaged maximum Nusselt number. Figure 8 shows the variation of the time-averaged maximum Nusselt number versus the Reynolds number and the diameter ratio, respectively, for a range of pulsation frequencies. The time-averaged maximum Nusselt number increases with the increase in Reynolds number for all pulsation frequencies. The increase is not significant but the trend is similar to the ones obtained for steady flows. Figure 9 shows the variation in the value of the maximum Nusselt number with the variation of diameter ratio d/D and Reynolds number for pulsating flow. As can be seen, as the diameter ratio increases, the value of the maximum Nusselt number decreases. The reduction in the Nusselt number values for larger diameter ratios may be attributed to the fact that as the diameter ratio increases recirculation zone diminishes. This results in less turbulence intensities downstream from the abrupt expansion, hence less heat transfer rates are expected. This trend is consistent with the steady-state results obtained by Eaton and Johnston (1981). Also in this case, the frequency of pulsation has almost negligible effect on the value of the maximum Nusselt number. The present calculations for the effect of the diameter ratio on the location of the reattachment point at different pulsation frequencies and Reynolds numbers indicate that, for a given Reynolds number, the location of the maximum Nusselt number moves downstream as the diameter ratio increases for all pulsation frequencies. Hence it exhibits the same trend as for steady-state case (Eaton and Johnston, 1981). The frequency of pulsation has no effect on the location of the reattachment point.

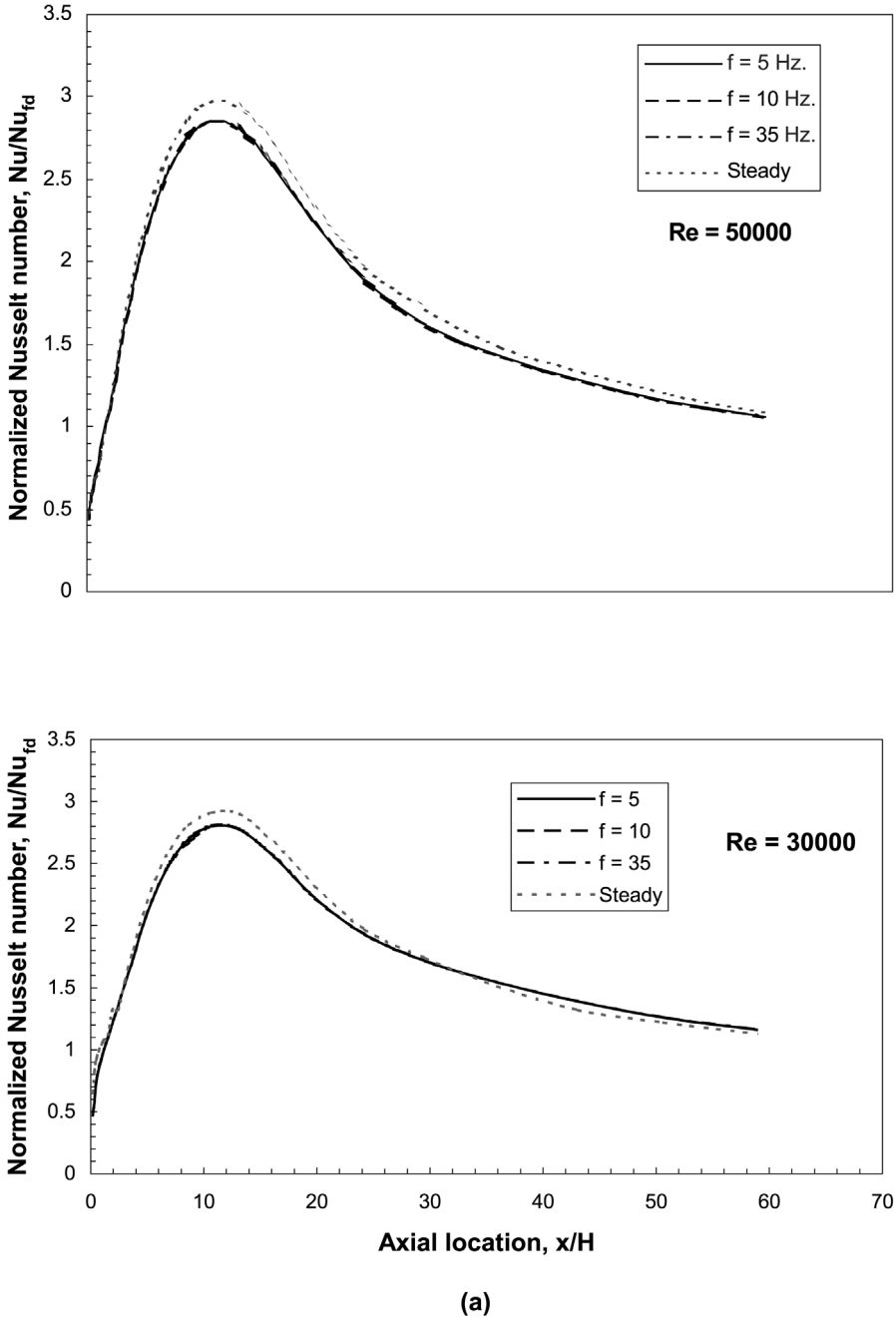

(continued)

Figure 7.
(a) Variation of local Nusselt number with axial location $d/D = 0.3$, $\alpha = 0.25$, and Pr = 0.7. (b) Variation of local Nusselt number with axial location $d/D = 0.3$, $\alpha = 0.25$, and Pr = 7.0

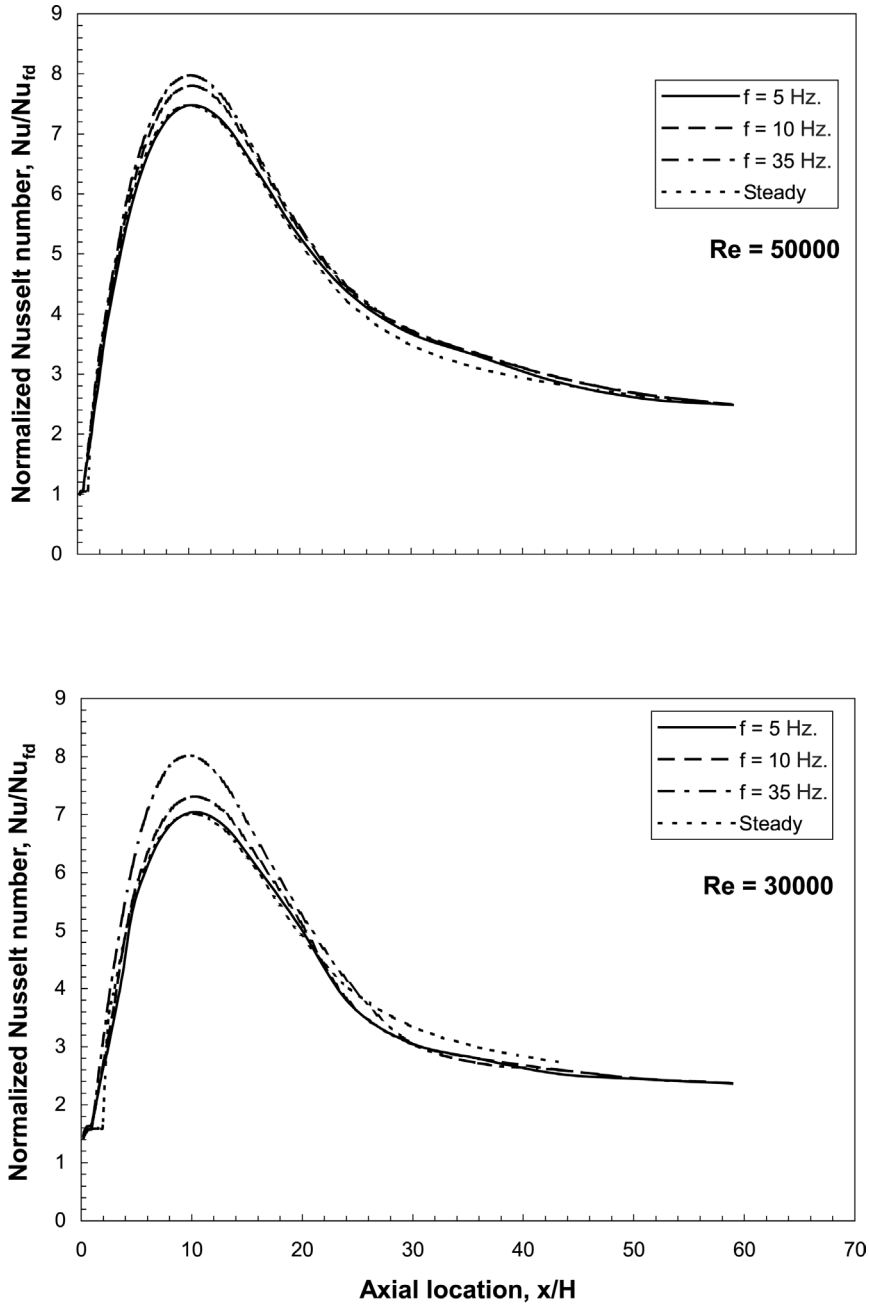
Normalized Nusselt number, Nu/Nu$_{fd}$
f = 5 Hz.
f = 10 Hz.
f = 35 Hz.
Steady
Re = 50000
Re = 30000
Axial location, x/H
0
1
2
3
4
5
6
7
8
9
10
20
30
40
50
60
70

(b)

Figure 7.

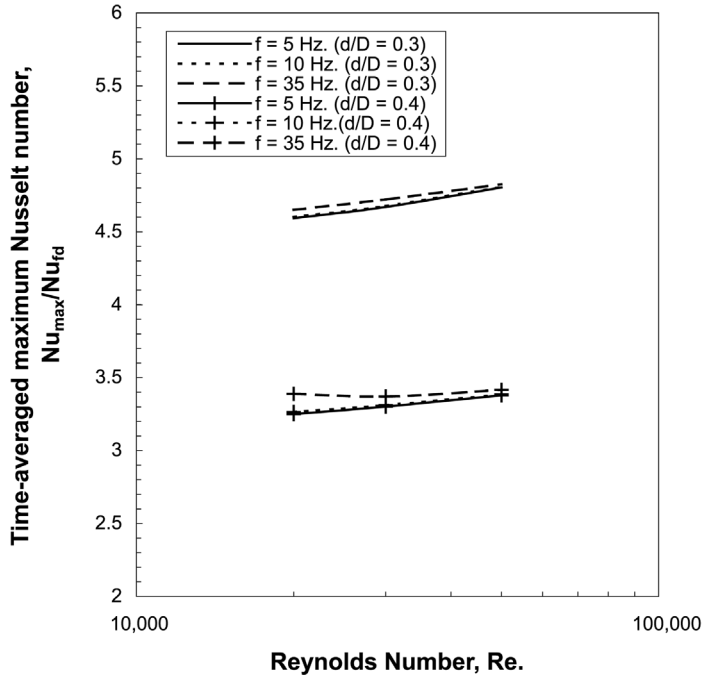

Figure 8.
Influence of Reynolds number on maximum Nusselt number at $\alpha = 0.25$, and $\mathrm{Pr} = 0.7$

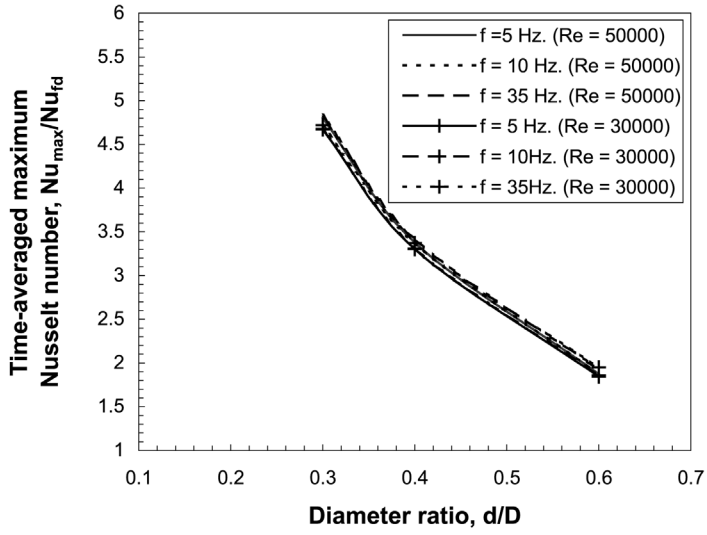

Figure 9.
Influence of diameter ratio (d/D) on maximum Nusselt number at different frequencies and at $\alpha = 0.25$, and $\mathrm{Pr} = 0.7$

The fourth set of results pertains to the effect of pulsation frequency on the value of heat transfer characteristics for different Prandtl numbers. As can be seen from Figure 10, the Nusselt number ratio increases linearly. The increase is very small ($\sim$5 per cent) in the frequency range being considered in this study

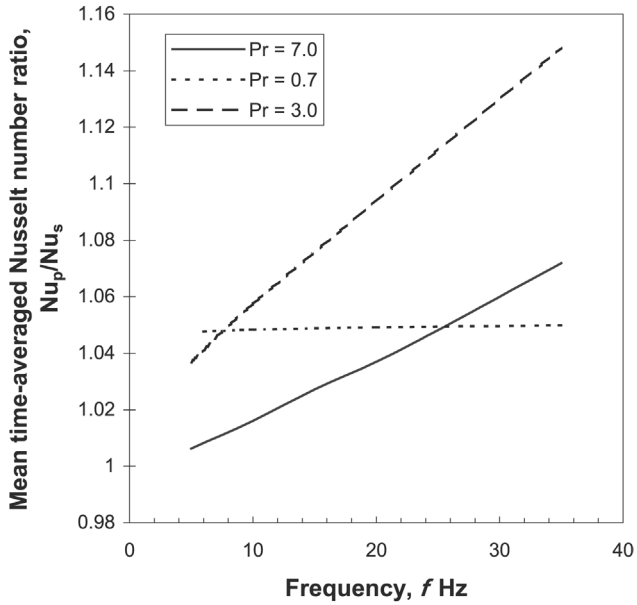

Figure 10.
Influence of frequency on the mean time-averaged Nusselt number ratio (Nu_p/Nu_s) at different Prandtl number and at d/D=0.5, Re = 50,000, and $\alpha = 0.25$

(5-35 Hz). As the Prandtl number increases, the rate of increase in the Nusselt number ratio becomes significant. There are different interpretations reported in the literature regarding the effect of pulsation frequency on the heat transfer rate. One interpretation is that the frequency of pulsation can greatly lower the critical Reynolds number (compared to steady flows) and steepens the velocity profile close to walls. This is likely to reduce the boundary layer thickness where heat transfer by viscous effect dominates. Hence an increase in turbulence intensity as well as the heat transfer coefficient is expected (Kastner and Shih, 1951). The second interpretation which is given by Valueva *et al.* (1994) indicates that in the case of quasi-steady turbulence (low frequency oscillations) with turbulent Stokes number $S_t \sim t/t_o \ll 1$, the turbulence succeeds in lining up with the instantaneous value of the Reynolds number at every instant of time, which in the case of a high-frequency range, the time scales of turbulence are much higher than the period of oscillations ($t/t_o \gg 1$) and the turbulence does not succeed in responding to time variations in the flow rate (the Reynolds number). For intermediate frequencies, force oscillations interact with turbulent pulsations, which increases the intensity of the latter and the heat transfer rates. The calculated results of the present study lie in the region of intermediate frequency range and increased rates of heat transfer are obtained.

The fifth set of results pertains to the effect of the Reynolds number on the mean time-averaged Nusselt number for the abrupt expansion ratios. The calculations are made for Prandtl numbers of 0.7 and 7.0 as shown in Figure 11(a)-(c), respectively. As can be seen from Figure 11(a) and (b),

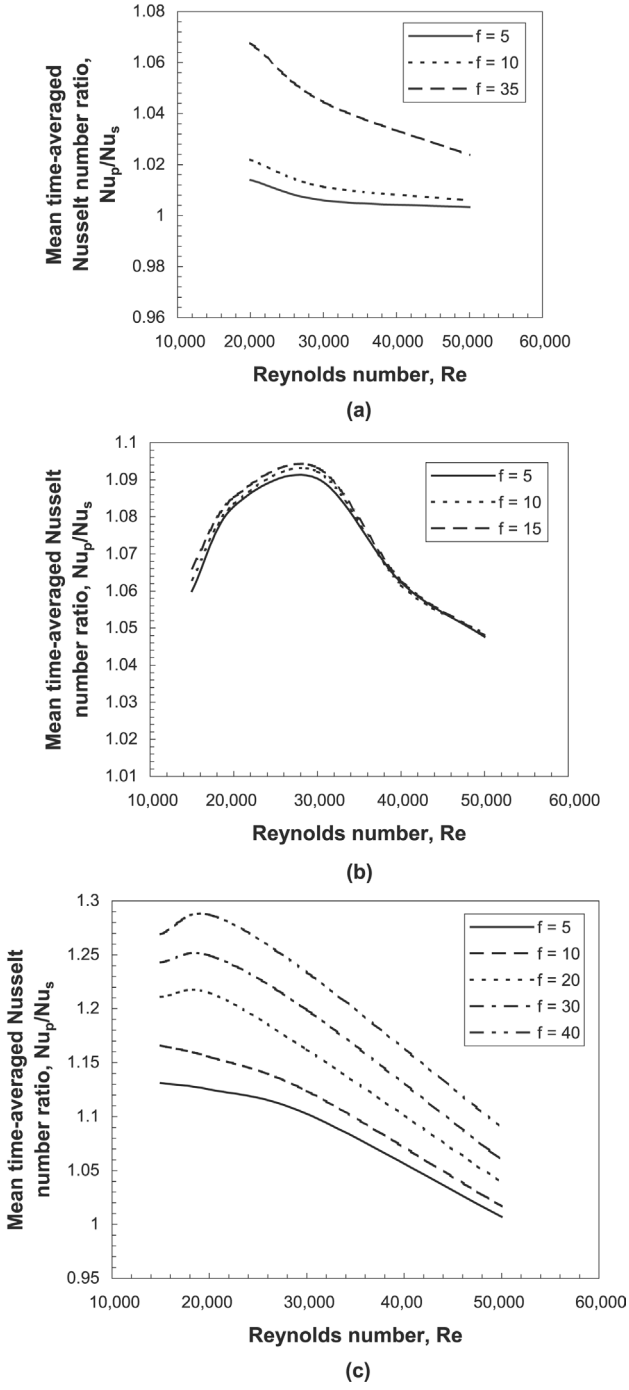

Figure 11.
(a) Influence of Reynolds number on the mean time-averaged Nusselt number (Nu_p/Nu_s) at different frequencies and at $\alpha = 0.25$, $Pr = 0.7$, and $d/D = 0.6$. (b) Influence of Reynolds number on mean time-averaged Nusselt number ratio (Nu_p/Nu_s) at different frequencies and at $\alpha = 0.25$, $Pr = 0.7$, and $d/D = 0.5$ (c) Influence of Reynolds number on the mean time-averaged Nusselt number ratio (Nu_p/Nu_s) at different frequencies and at $d/D = 0.5$, $\alpha = 0.25$, and $Pr = 7.0$

the Nusselt number ratio (Nu_p/Nu_s) decreases with increase in Reynolds number except for a diameter ratio of 0.5 where the ratio of the Nusselt number increases to a maximum value at certain Reynolds numbers and then gradually decreases upon further increase in the Reynolds number. This feature is clearly indicated in Figure 11(c) in case of the high Prandtl numbers. Figure 12 shows variation of Nu_p/Nu_s with the diameter ratio for frequencies of 5, 10, and 35 Hz and Reynolds numbers of 30,000 and 50,000. As can be seen, the Nusselt number ratio increases as the diameter ratio increases. It reaches a peak value at a diameter ratio of 0.5 and then decreases for further increase in the diameter

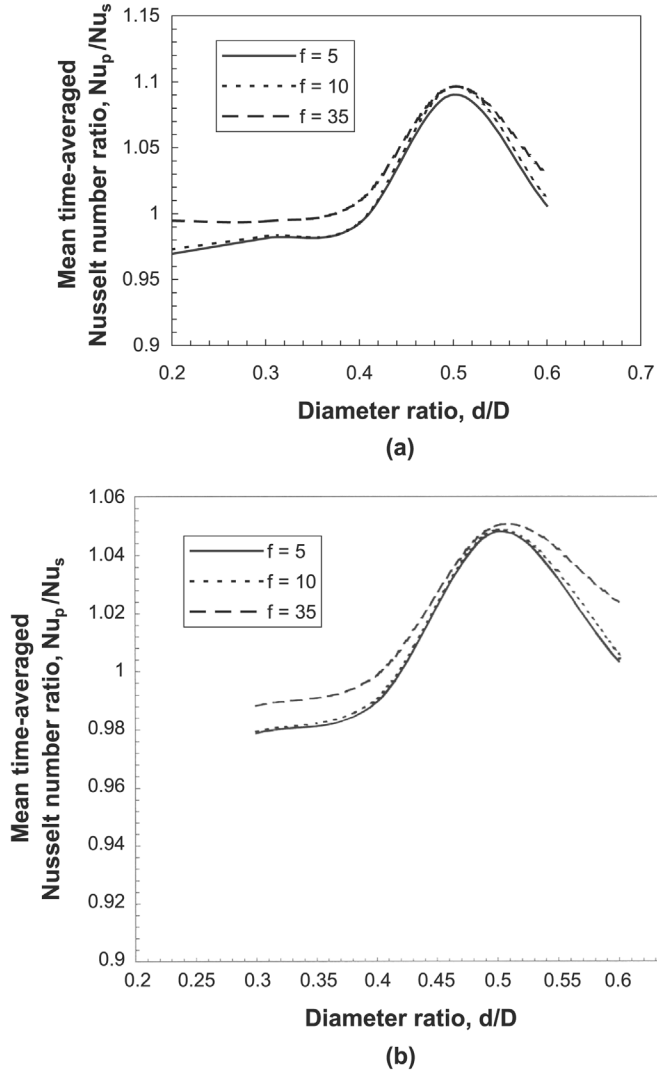

Figure 12.
(a) Influence of diameter ratio (d/D) on mean time-averaged Nusselt number (Nu_p/Nu_s) at $\alpha = 0.25$, $Pr = 0.7$, and $Re = 30{,}000$.
(b) Influence of diameter ratio (d/D) on mean time-averaged Nusselt number (Nu_p/Nu_s) at $\alpha = 0.25$, $Pr = 0.7$, and $Re = 50{,}000$

ratio. Also the values of the Nusselt number ratio increase with the increase in pulsation frequency.

Turbulence intensities downstream from the abrupt expansion vary inversely with the diameter ratio (d/D) (Eaton and Johnston, 1981). Therefore, it may be concluded that for a given frequency and diameter ratio, as the Reynolds number increases the turbulence downstream the abrupt expansion increases and becomes frozen. Hence, no significant variation in heat transfer rates are expected. For the diameter ratio of 0.5, Nu_p/Nu_s increases to a maximum and then decreases with further increase in the Reynolds number. Increase in the Nu_p/Nu_s with the Reynolds number may be attributed to the fact that the first half of the curve could be related to the intermediate frequency range where increase in Nu_p/Nu_s is expected, whereas, the second half of the curve could be related to the region of high frequency where Nu_p/Nu_s decreases to a steady-state value. The behaviour of the Nusselt number with diameter ratio can be explained in view of the bursting phenomena using the turbulent bursting model (Genin *et al.*, 1992; Liao and Wang, 1985). This model defines certain regions on the frequency-Reynolds number plane such that depending on the region in this plane, the bursting frequency can be dependent or independent of the pulsation frequency (Habib*et al.*, 1999). According to the results of Habib *et al.* (1999), Mamayev *et al.* (1976) and Liao and Wang (1985), heat transfer can be increased or decreased with Reynolds number and frequency. The diameter ratio influences to a large extent the bursting frequency and consequently the influence of the Reynolds number on the Nusselt number as a result of change in both the reattachment length and the size of the recirculation zone. For small diameter ratio ($d/D < 0.5$) turbulence downstream from an abrupt expansion dominates and imposed pulsation frequency has negligible effect on heat transfer rates. As the diameter ratio increases towards 0.5, the turbulence downstream from the abrupt expansion diminishes and imposed pulsation frequency enhances the turbulence. Hence the heat transfer rate increases.

The sixth set of results pertains to the effect of the Prandtl number on the mean time-averaged Nusselt number at different pulsation frequencies. Figure 13 shows the variation of the Nusselt number ratio with the Prandtl number at a Reynolds number of 50,000. As can be seen from the figure, the Nusselt number increases with the Prandtl number reaching a maximum value at a Prandtl number of 2.0 and then decreases as the Prandtl number increases for all frequencies. The Nusselt number values increase slightly as the pulsating frequency increases. In relation to the influence of the Prandtl number, two opposing effects may be considered. The first is that as the Prandtl number increases, the flow tends to laminarize and consequently, an increase in the boundary-layer thickness occurs through which heat is transferred on a molecular scale. On the other hand, an increase in the Prandtl number causes the influence of pulsation on heat transfer characteristics to

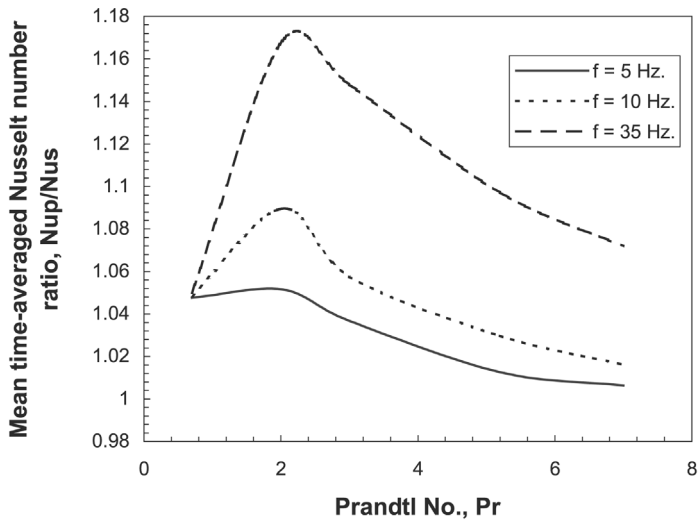

Figure 13.
Influence of Prandtl number on the mean time-averaged Nusselt number ratio (Nu_p / Nu_s) at different frequencies and at Re=50,000, $\alpha = 0.25$, and $d/D = 0.5$

become significant. The balance between these two effects is likely to be the reason for the increase in heat transfer as the Prandtl number increases to $Pr = 2.0$ which is followed by a reduction in heat transfer at a higher Pr. This is also confirmed by Figure 10 described earlier.

Conclusions

- At all pulsation frequencies the variation in mean time-averaged Nusselt number, maximum Nusselt number and its location with Reynolds number and diameter ratio exhibit similar trends to steady flows.
- Frequency has insignificant effect on the values of mean time-averaged Nusselt number for a Prandtl number of 0.7 (the maximum increase in the mean time-averaged Nusselt number ratio is approximately 10 per cent at the frequency of 35 Hz and $Re = 30,000$). Whereas, the effect of pulsation frequency is appreciable for fluids having a Prandtl number greater than 1.0 (maximum rise of about 30 per cent is indicated in the mean time-averaged Nusselt number ratio for a Prandtl number of 7.0 at the frequency of 40 Hz and a Reynolds number of 20,000).
- An increase in the Reynolds number results in the decrease of the mean time-averaged Nusselt number ratio for all pulsation frequencies and diameter ratios. An interesting behaviour is indicated for the diameter ratio of 0.5. The values of the mean time-averaged Nusselt number ratio increases as the Reynolds number increases, reaches a peak, and then decreases for further increase in the Reynolds number for all pulsation frequencies. Similar characteristics are obtained for a Prandtl number of 7.0 as well.

- For all pulsation frequencies, as the diameter ratio increases the values of mean time-averaged Nusselt number ratio increases. It reaches a peak at a diameter ratio of 0.5 and then decreases for further increase in the diameter ratio.

References

Amano, R.S. (1983), "A study of turbulent flow downstream of an abrupt pipe expansion", *AIAA Journal*, Vol. 21, pp. 1400-5.

Amano, R.S., Jenson, M.K. and Geol, P. (1983), "A numerical and experimental investigation of turbulent transport downstream from an abrupt pipe expansion", *Journal of Heat Transfer*, Vol. 105, pp. 862-9.

Baughn, J.W., Hoffman, M.A., Takahashi, R.K. and Daehee, L. (1987), "Heat transfer downstream of an abrupt expansion in the transition Reynolds number regime", *Journal of Heat Transfer*, Vol. 109, pp. 37-42.

Baughn, J.W., Hoffman, M.A., Takahashi, R.K. and Launder, B.E. (1984), "Local heat transfer downstream of an abrupt expansion in a circular channel with constant wall heat flux", *Journal of Heat Transfer*, Vol. 106, pp. 789-95.

Baughn, J.W., Hoffman, M.A., Launder, B.E., Daehee, L. and Yap, C. (1989), "Heat transfer, temperature and velocity measurements downstream of an abrupt expansion in a circular tube at a uniform temperature", *Journal of Heat Transfer*, Vol. 111, pp. 870-6.

Chieng, C.C. and Launder, B.E. (1980), "On the calculation of turbulent heat transport downstream from an abrupt pipe expansion", *Numerical Heat Transfer*, Vol. 3, pp. 189-207.

Cho, H.W. and Hyun, J.M. (1989), "Motion and heat transfer in the Blasius flow containing a pulsating component", *International Journal of Heat and Fluid Flow*, Vol. 10 No. 4, pp. 349-56.

Dallen back, P.A., Metzger, D.E. and Neitzel, G.P. (1987), "Heat transfer to turbulent swirling flow through a sudden axisymmettric expansion", *Journal of Heat Transfer*, Vol. 109, pp. 613-20.

Eaton, J.K. and Johnston, J.P. (1981), "A review of research on subsonic turbulent flow reattachment", *AIAA Journal*, Vol. 19 No. 9, pp. 1093-100.

Genin, L.G., Koval, A.P., Manchkha, S.P. and Sviridow, V.G. (1992), "Hydrodynamics and heat transfer with pulsating fluid flow in tubes", *Thermal Engineering*, Vol. 39 No. 5, pp. 30-4.

Habib, M.A. and McEligot, D.M. (1982), "Turbulent heat transfer in a swirl flow downstream of an abrupt expansion", *The Seventh International Heat Transfer Conference*, Munchen, Fed. Rep. of Germany, Hemisphere Publishing Corporation, FC29, pp. 159-64.

Habib, M.A. and Whitelaw, J.H. (1980), "Velocity characteristics of confined coaxial jets with and without swirl", *Journal of Fluids Engineering*, Vol. 102, pp. 47-53.

Habib, M.A., Said, S.A.M., Al-Dini, S.A., Asghar, A. and Gbadebo, S.A. (1999), "Heat transfer characteristics of pulsated turbulent pipe flow", *Journal of Heat and Mass Transfer*, Vol. 34 No. 5, pp. 413-21.

Hammad, K.J. and Vrandis, G.C. (1998), "Asymptotic flow regimes pulsatile flows of Bingham plastics", *Journal of Fluids Engineering*, Vol. 120, pp. 211-3.

Kastner, L.J. and Shih, S.H. (1951), "Critical Reynolds number for steady and pulsating flow", *Thermal Engineering*, pp. 389-91.

Kim, S.Y. and Yang, B.H. (1998), "Forced convection heat transfer from two heated blocks in pulsating channel flow", *International Journal of Heat and Mass Transfer*, Vol. 41 No. 4, pp. 625-34.

Krall, K.M. and Sparrow, E.M. (1966), "Turbulent heat transfer in the separated, reattached, and redevelopment regions of a circular tube", *Journal of Heat Transfer*, Vol. 88 No. 1, pp. 131-6.

Liao, M.S. and Wang, C.C. (1985), "An investigation of heat transfer in pulsating turbulent pipe flow. ASME, fundamentals of forced and mixed convection", *The 23rd National Heat Transfer Conference*, 4-7 August 1985, Denver, CO, pp. 53-9.

Mamayev, V.V., Nosov, S. and Syromyatnikov, I. (1976), "Investigation of heat transfer in pulsed flow of air in pipes", *Heat Transfer – Soviet Research*, Vol. 8 No. 3, pp. 111-6.

Patankar, S.V. (1980), *Numerical Heat Transfer and Fluid Flow*, McGraw-Hill, NY.

Rodi, W. (1984), "Turbulence models and their applications in hydraulics", *State of Art Paper. International Association of Hydraulic Research*, 2nd ed., University of Karlsruhe, Karlsruhe, FRG.

Stieglmer, Tropea, C.M., Weiser, N. and Nitsche, W. (1989), "Experimental investigation of the flow through axisymmetric expansion", *Journal of Fluids Engineering*, Vol. 111, pp. 464-71.

Valencia, A. and Hinojosa, L. (1997), "Numerical solution of pulsating flow and heat transfer characteristics in a channel with backward facing step", *Heat and Mass Transfer*, Vol. 32 No. 3, pp. 143-8.

Valencia, A., Fiebig, M. and Mitra, N.K. (1996), "Heat transfer enhancement by longitudinal vortices in a fin-tube heat exchanger with flat tubes", *Journal of Heat Transfer*, Vol. 118 No. 1, pp. 209-11.

Valueva, E.P., Popov, V.N. and Romanov, S.Y. (1994), "Heat transfer in pulsating turbulent flow in a round tube", *Thermal Engineering*, Vol. 41 No. 3, pp. 182-93.

Versteeg, H.K. and Malalasekera, W. (1995), *An Introduction to Computational Fluid Dynamics; The Finite Volume Method*, Longman Scientific and Technical, London.

Vogel, J.C. and Eaton, J.K. (1985), "Combined heat and fluid dynamic measurements downstream of a backward facing step", *Journal of Heat Transfer*, Vol. 107, pp. 922-9.

Zemanic, P.P. and Dougall, R.S. (1970), "Local heat transfer downstream of abrupt circular channel expansion", *Journal of Heat Transfer*, Vol. 92, pp. 53-60.